000012

Kinetic Monte–Carlo Modeling of hydrogen retention and re–emission from Tore–Supra deposits

* A. Rai[a], R. Schneider [a], M. Warrier [b], P. Roubin [c], C. Martin [c], and M. Richou [c]

[a] *Max-Planck-Institut für Plasmaphysik, D-17491 Greifswald, Germany*

[b] *Computational Analysis Division, BARC, Trombay, Mumbai, India - 400085*

[c] *PIIM, Université de Provence, Centre Saint–Jérôme (service 242) F–13397 Marseille cedex 20, France*

Abstract :A multi–scale model has been developed to study the reactive–diffusive transport of hydrogen in porous graphite [1]. The deposits found on the leading edge of the neutralizer of Tore Supra are multi–scale in nature, consisting of micropores with typical size lower than 2 nm ($\sim 11\%$), mesopores ($\sim 5\%$) and macropores with a typical size more than 50 nm [2]. Kinetic Monte–Carlo (KMC) has been used to study the hydrogen transport at meso–scales. Recombination rate and the diffusion coefficient calculated at the meso–scale was used as an input to scale up and analyze the hydrogen transport at macro–scale. A combination of KMC and MCD (Monte–Carlo Diffusion) method was used at macro–scales. Flux dependence of hydrogen recycling has been studied. The retention and re–emission analysis of the model has been extended to study the chemical erosion process based on the Küppers–Hopf cycle [3].

keywords: Graphite, Diffusion, Hydrogen, First wall materials.

* *Corresponding author e–mail:* Abha.Rai@ipp.mpg.de

1 Introduction

Tritium retention is a key issue to be investigated for the next step fusion devices using carbon walls. Tore Supra offers a unique opportunity to study the steady–state particle balance due to its ability to produce long discharges (>200 s) [4]. In long pulses, particle balance gives evidence that a constant fraction of the injected gas (typically 50% of the injected fuel) is retained in the wall for the duration of the shot, showing no sign of wall saturation after more than 6 minutes of discharge [5]. Extrapolation of these results for ITER leads to an unacceptable value of tritium retention levels in the machine. In addition to this, the ratio of D/C in the deposits collected from TS neutralizer deposits is $< 1\,\%$ [6]. Neither implantation nor co–deposition could explain the constant retention rates observed in Tore Supra. It was speculated that the implantation of the hydrogen followed by the diffusion through the internal porosity could lead to the penetration and trapping of the hydrogen much deeper than expected on the basis of depth of penetration, into the graphite used as plasma facing components (PFC). This gives rise to the need for a better understanding of the transport, retention and re–emission of hydrogen into the co–deposited layers and into the graphite.

2 Structure of the Tore Supra deposits

Based on the experimental structural analysis [2], we simulate the hydrogen retention and re-emission of the deposits found on the leading edge of the neutralizer

(named N-LE) of Tore Supra. The typical plasma flux near this region is about $10^{17} - 10^{18}$ $D^+cm^{-2}s^{-1}$ and the temperature can reach up to 1500 K. The incident ion energy near the neutralizer region is typically 50 – 300 eV. The location of these deposits is in the direct line–of–sight of the plasma (under the toroidal limiter). The deposits were analyzed using adsorption isotherm measurements and electron microscopy. At this location the field lines are almost perpendicular to the surface and the deposited layers grows in ovoid–shaped structures, elongated along a direction close to that of the magnetic field [4]. It was found that the neutralizer deposits show a high specific surface area (around 190 m^2g^{-1}) [2]. They consist of small graphite like crystallites whose typical sizes are 2–4 nm and 7–9 nm parallel and perpendicular to the graphene planes respectively [7,8]. The porosity of these deposits is multiscale in nature consisting of micropores with typical size lower than 2 nm ($\sim 11\%$), mesopores (typical size between 2 and 50 nm, $\sim 5\%$) and macropores with a typical size more than 50 nm. Transmission electron microscopy performed on thin foils cut from an ovoid reveals a regular network of parallel slit–shaped mesopore (size $\sim$ 10 nm) and macropores (size $\sim$ 100 nm), with a well–defined orientation with respect to the ovoid axis.

3 Model

In the earlier work hydrogen isotope diffusion in porous graphite was modeled using a time dependent, 3-dimensional, multi-scale model [9–11]. The model used molecular dynamics (MD) at the micro-scales ($2.5\ nm, 10^{-10}\ s$) and consistently parametrized

the MD results within a KMC scheme [10]. The KMC scheme was extended to include trapping–detrapping at the crystallite-micro-void interface and molecule formation using Smoluchowski boundary condition [12] to simulate trans-granular-diffusion (TGD) at the meso-scales (10^{-7} m, several ms) [11]. The results from our micro-scale modeling and from experiments ([13] and references therein) were used as inputs in KMC scheme. This concept was then extended to the macro-scales (10^{-2} m, up to a few *seconds*), by using the parametrized TGD diffusion co-efficient in a Monte Carlo diffusion model with transport in voids using a KMC model, thereby having a truly multi-scale capability [9]. The other details of the model and various processes included in the model can be found in [1].

As an improvement to the model where only a predefined number of hydrogen atoms were simulated, a true steady state with a continuous influx of hydrogen atoms determined by the flux of the ion beam has been implemented. This improvement in the code allows us to understand the effect of the different particles arriving at different times in the simulation and the effect of this on their diffusion and recombination processes. The complete model of the chemical erosion based on the Küppers–Hopf cycle [3] has been implemented. This will allow us to study the flux dependence of the chemical erosion of graphite sample having different internal structures.

In the present work we use the following nomenclature for different length scales:

- micro–scales: void size $< 2 \times 10^{-9}$ m and system dimension of several 10^{-9} m.
- meso–scales: void size $< 10 \times 10^{-9}$ m and system dimension of several 10^{-7} m.
- macro–scales: void size $> 50 \times 10^{-9}$ m and system dimension of several 10^{-6} m.

We parametrized the recombination rate and TGD coefficient for the TS deposits at meso–scales (sample having micropore and mesopores) and used them as input to model macropores at macro–scales.

4 Setting up the simulation

At meso–scales, the geometry was implemented in our simulations by creating a porous structure of $3 \times 10^{-7}\,m$, $3 \times 10^{-7}\,m$, $1 \times 10^{-7}\,m$ in X, Y and Z direction respectively, representing a typical granule with periodic boundary conditions in X and Y direction. The basic cell size was $1 \times 10^{-9}\,m$. The graphite sample was composed of micropores having 11% void fraction with void size $1 \times 10^{-9}\,m$, $1 \times 10^{-8}\,m$, $1 \times 10^{-8}\,m$ and mesopores having 5% void fraction with void size $1 \times 10^{-8}\,m$, $1.8 \times 10^{-8}\,m$, $1.8 \times 10^{-8}\,m$ in X, Y and Z directions respectively. Out of the total 9×10^{6} cells in the simulation box $\sim 21\%$ are surface cells. We are interested in the analysis of thermalized hydrogen. The ion beam energy we have considered in our simulation is 300 eV. We approximate the profile of the ions given by TRIM calculations to a Gaussian distribution with a range of penetration of $7.5 \times 10^{-9}\,m$ and a standard deviation of $6.0 \times 10^{-9}\,m$ along the z–direction. The deposits have 0.75 % active carbon sites, therefore, in our simulation, every time an atom jumps, a trapping probability of 0.0075 is used.

At macro–scales, the geometry was implemented in our simulations by creating a porous structure of $2 \times 10^{-6}\,m$, $2 \times 10^{-6}\,m$, $2 \times 10^{-6}\,m$ in X, Y and Z direction respectively, with periodic boundary conditions in X and Y direction. The basic cell size

was $1 \times 10^{-8}\, m$. The graphite sample was composed of macropores having 10% void fraction with void size $1 \times 10^{-7}\, m$, $1 \times 10^{-7}\, m$, $6 \times 10^{-7}\, m$. For the hydrogen atom and molecule transport, KMC was used in the voids and MCD was used in the granules.

5 Results

Fig.1 shows the recombination rate for different incident fluxes ranging from $10^{17}\, H/m^2/s$ (ion beam experiments) to $10^{24}\, H/m^2/s$ (plasma fusion devices) as a function of target temperature. Note that for the lower fluxes, there is a peak recombination rate and this peak shifts to higher temperatures as the flux increases. It is also seen that on an average, the recombination rate increases with increasing flux. At higher incident fluxes there is no peak. This can be understood as follows: the recombination rate depends on two factors: (i) It increases with increasing H density in the sample and (ii) It increases with increased diffusion coefficient of H in the sample. At a given incident flux, the density decreases with temperature tending to decrease the recombination rate and the diffusion coefficient increases with temperature tending to increase the recombination rate. This balance is what leads to a maxima in the recombination rates as the temperature is increased. It is obvious that the density of H increases with increasing flux. Therefore at higher fluxes, the diffusion contribution to recombination rate matches the decreasing density contribution only at higher temperatures and the maxima in the recombination rate peak shifts to higher temperatures. At very high fluxes, diffusion does not affect the recombination rate due to high densities and a

maxima does not show up.

In ion–beam experiments the graphite samples which are used have void fraction $\simeq$ 10% and void sizes of the order of nano–meters and therefore the samples are saturated after a fluence of $\simeq 10^{17}\, H/m^2$ and 100% re–emission is observed [1]. Whereas for Tore Supra deposits due to the very large voids the hydrogen atoms can penetrate much deeper via diffusion along the internal surfaces and therefore, no re–emission was observed. At temperatures of about 1200–1500 K, the retained amount was around 50% [4]. In our simulations too, even after very long time ($\simeq 10^{-2}\, s$) the sample was not completely saturated and the retention level depends on the incident flux.

Fig.2 shows the effect of the incident flux on the hydrogen retention. We see that at temperatures $<$ 1000 K, most of the incident flux is retained. At higher temperatures there is a drop in the retained fraction, with lower fluxes showing the drop at temperatures lower than those with higher fluxes. As the flux increases, at a given temperature $>$ 1000 K, it is seen that larger fraction of the incident flux is retained. At temperatures $<$ 1000 K, the hydrogen densities are high, and there is low probability of H atomic desorption and detrapping due to their higher activation energy compared to diffusion in crystallites (activation energy $\sim$ 0.015, 0.28 eV). The H atoms recombine within crystallites mostly and the H_2 molecule formed has a high migration energy in crystallites. Therefore we observe high values of retained fraction. As the temperature increases above 1000 K, we observe the trends seen in Fig.2., i.e. at lower fluxes

the recombination rates are lower. The probabilities of other mechanisms of hydrogen loss (atomic desorption, detrapping) increase whereas that of recombination decreases. Therefore at lower incident fluxes we see lesser retained fraction of incident flux. Due to the size of the hydrogen molecules, their migration energy in the inter-layer spacing of graphite crystals is high. This acts as a sink for the hydrogen at high fluxes. For flux of $10^{24}\,H/m^2/s$ even at for surface temperature as high as 2000 K, 50% of hydrogen is still retained in the sample. This is also consistent with the observation by Haasz et al. [14], wherein the temperature at which both atomic and molecular hydrogen are released in equal amount ($T_{50\%}$) shifts towards higher temperatures by increasing the flux and a large fraction of molecules are released even at higher temperatures.

Fig.3 shows the retained amount of hydrogen at meso–scales (sample having micro–pores and meso–pores together) and macro–scales (sample having macropores) from Tore Supra deposits subjected to flux of $10^{20}\,H/m^2/s$. It must be noted that the fraction of hydrogen retained by micropores and mesopores till 1600 K is $\simeq$ 90% whereas for macropores it is around 60 %. This implies that the macopores play a dominant role for the release of hydrogen. This is due to the fact that at the macro–scale the structure consists of bulk (which contains the effect of micropores and mesopores having 16% void fraction) separated by macropores (10% void fraction). So the structure at the macro–scale has higher internal porosity which makes the access to the macropores and eventually the geometrical surface easier. At 2000 K, the retention level drops to zero for mesopores whereas 10 % hydrogen is still retained in the macropores. This could be possible if some of the hydrogen which is released from the mesopores get

trapped at the macropore surfaces. This gives rise to an internal inventory (or deposition) on macropore surfaces. This mechanism might play a very significant role during the chemical sputtering of such deposits. In that case we might see the deposition of the hydrocarbons on the internal surfaces of the macropores. This would further enhance the tritium retention problem.

Fig.4 shows the hydrogen release behavior for mesopores and macropores. From the total released amount the fraction contributed by atoms and molecules is plotted on the Y–axis. The retained amount for these two cases are given in Fig.3 and one can find for each temperature the exact amount of hydrogen released from the retained amount ($(100 - \textit{retained amount}\,(\%)\,) \times 100$). At meso–scales, The hydrogen release curve follows the experimental results of [15] and the model calculation of [14], *i.e.* the released flux is mainly molecular hydrogen at lower temperatures and atomic hydrogen at higher temperatures and has been explained earlier [1]. At macro–scales, all the hydrogen atoms which are distributed on the macropore surfaces, are trapped (high trapping probability of 0.0075) or they diffuse deep into the bulk. The hydrogen atoms which land up in the granules diffuse within it (MCD, using TGD coefficient) and get recombined to form hydrogen molecules (determined by the recombination rate calculated at meso–scales). As explained above, all the hydrogen released in the atomic from the mesopores get trapped again at the macropores surfaces. The hydrogen which is released in the molecular form from the mesopores, due to its chemical inactivity is able to reach the geometrical surface and get released from there. Therefore, at macro–scales even at very high temperatures hydrogen is released mainly in the molecular

form.

Fig.5 shows the profile of the hydrogen present in different chemical state (adsorbed, trapped) at the macro–scales. It can be seen that most of the hydrogen is either adsorbed (0.9 eV) or trapped (2.67 eV) on the macropore surfaces. A large quantity of hydrogen is able to diffuse well beyond the implantation range ($7.5 \times 10^{-9}\, m$).

6 Residence time

The average time spent by a hydrogen atom in graphite (Residence time) was calculated and it depends on the temperature of the sample and the incident flux. The molecular diffusion is very fast, therefore, the residence time of hydrogen coming out as molecules is much lesser than the residence time of hydrogen released as atoms. At meso–scales, for ion–beam experiment fluxes ($\simeq 10^{17}\, H/m^2/s$) and 1200 K, the typical residence time is around $10^{-3}\, s$ for atoms and $10^{-10}\, s$ for solute hydrogen molecules. With increasing flux to $10^{20}\, H/m^2/s$, at 1200 K, the residence time is $10^{-10}\, s$ for atoms and $10^{-10}\, s$ for solute hydrogen molecules. At macro–scales no atoms are released at 1200 K and the residence time is around $10^{-7}\, s$ for molecules.

7 Summary and conclusions

The multi–scale model has been extended to simulate the steady–state reactive–diffusive transport of hydrogen in porous graphite. In the present work, the model

was used to study the hydrogen retention and release from Tore Supra deposits. At very high fluxes a large quantity of hydrogen molecules get stuck in the graphene planes and this acts as a sink for the hydrogen. The accumulation of the hydrogen on the surfaces of the macropores might lead to high tritium retention levels.

8 Acknowledgments

R. Schneider and A. Rai acknowledge funding of the work by the Initiative and Networking Fund of the Helmholtz Association. M. Warrier acknowledges funding from the Max-Planck India Fellowship.

References

[1] A. Rai, R. Schneider and M. Warrier, To be published in *J. Nucl. Mater.* http://dx.doi.org/10.1016/j.jnucmat.2007.08.013

[2] C. Martin, M. Richou, W. Sakaily, B. Pégourié, C. Brosset and P. Roubin, *J. Nucl. Mater.* 363-365 (2007) 1251-1255.

[3] M. Wittmann and J. Küppers, *J. Nucl. Mater.* 227 (1996) 186.

[4] B. Pégourié, C. Brosset, E. Delchambre, T. Loarer, P. Roubin, E. Tsitrone, J. Bucalossi, J. Gunn, H. Khodja, C. Lafon, C. Martin, P. Parent, R. Reichle and Tore Supra Team, *Physics Scripta* T111 (2004) 23-28.

[5] E. Tsitrone, D. Reiter, T. Loarer, C. Brosset, J. Bucalossi, L. Begrambekov, C. Grisolia,

A. Grosman, J. Gunn, J. Hogan, et al., *J. Nucl. Mater.* 337-339 (2005) 539-543.

[6] C. Brosset and H. Khodja, *J. Nucl. Mater.* 337-339 (2005) 664-668.

[7] P. Roubin, C. Martin, C. Arnas, Ph. Colomban, B. P*égourié* and C. Brosset, *J. Nucl. Mater.* 337-339 (2005) 990-994.

[8] M. Richou, C. Martin, P. Roubin, P. Delha*és*, M. Couzi, C. Vix-Guterl, J. Dentzer, W. Saikaly, C. Brosset, B. P*égourié*, A. Litnovsky, V. Philipps, P. Wienhold, To be published in *Carbon* (2007)

[9] M. Warrier, R. Schneider, E. Salonen, and K. Nordlund. *J. Nucl. Mater.*, 337-339, (2005) 580.

[10] M. Warrier, R. Schneider, E. Salonen, and K. Nordlund. *Physica Scripta*, T108 (2004) 85.

[11] M. Warrier, R. Schneider, E. Salonen, and K. Nordlund. *Contrib. Plasma Phys.*, 44(1-3), (2004) 307.

[12] M. V. Smoluchowski. *Z. physik. Chem.*, 92, (1917) 192.

[13] K. L. Wilson et. al. *Atomic and plasma-material interaction data for fusion (supplement to the journal Nuclear Fusion*, 1, (1991) 31.

[14] A. A. Haasz, P. Franzen, J. W. Davis, S. Chiu, and C. S. Pitcher. *J. Appl. Phys.*, 77(1) (1995)66.

[15] P. Franzen and E. Vietzke, *J. Vac. Sci. Technol. A* 12 (1994) 820.

9 Figure captions

Fig. 1: Recombination rates from meso–scales as a function of temperatures for different incident fluxes. The flux value for Curves are ($1 \rightarrow\ 10^{17}\, H/m^2/s$, $2 \rightarrow\ 10^{20}\, H/m^2/s$, $3 \rightarrow\ 10^{21}\, H/m^2/s$, $4 \rightarrow\ 10^{22}\, H/m^2/s$, $5 \rightarrow\ 10^{24}\, H/m^2/s$).

Fig. 2: Retained amount of hydrogen from meso–pores as a function of temperatures for different incident fluxes. The flux value for Curves are ($1 \rightarrow\ 10^{17}\, H/m^2/s$, $2 \rightarrow\ 10^{20}\, H/m^2/s$, $3 \rightarrow\ 10^{22}\, H/m^2/s$, $4 \rightarrow\ 10^{24}\, H/m^2/s$).

Fig. 3: Retained amount of hydrogen for mesopores (curve 1) and macropores (curve 2). The incident flux was $10^{20}\, H/m^2/s$.

Fig. 4: Released amount of hydrogen atoms and molecules as a function of temperature for mesopores and macropores. Hydrogen atoms and molecules for mesopores are represented by curve 1 and 2 respectively. Similarly, for macropores hydrogen atoms and molecules are represented by curve 3 and 4 respectively.

Fig. 5: Profile of hydrogen present in different chemical state along the Z–direction. 1 $\rightarrow$ trapped hydrogen (2.67 eV), 2 $\rightarrow$ adsorbed hydrogen (0.9 eV), 3 $\rightarrow$ two trapped hydrogen close enough to form a molecule (2.3 eV), 4 $\rightarrow$ H_2 molecules in the void and 5 $\rightarrow$ H_2 molecules in the crystallites.

10 Figures

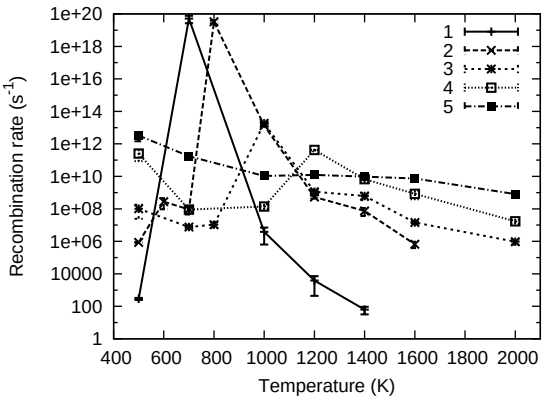

Fig. 1.

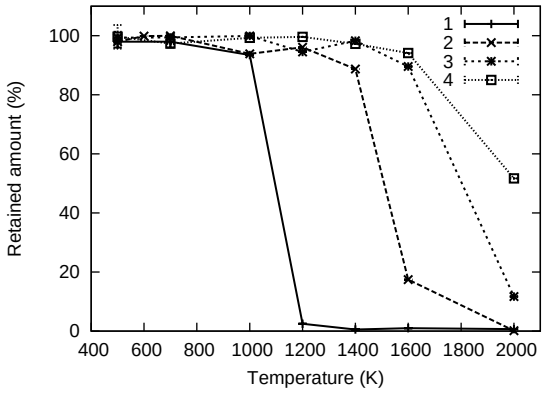

Fig. 2.

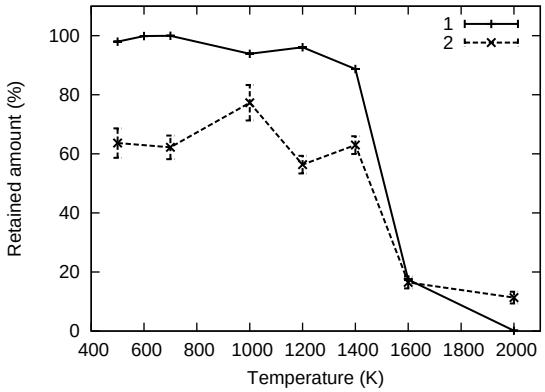

Fig. 3.

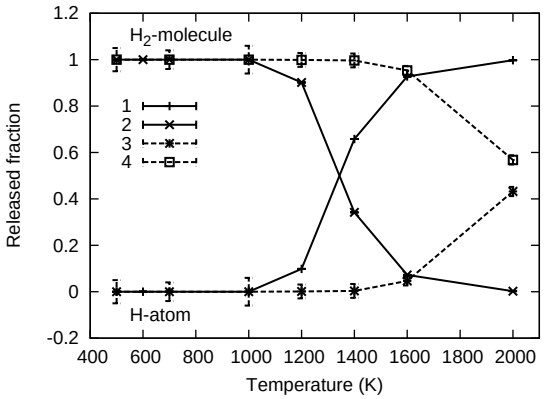
H2-molecule
H-atom
1
2
3
4
Released fraction
Temperature (K)
1.2
1
0.8
0.6
0.4
0.2
0
-0.2
400
600
800
1000
1200
1400
1600
1800
2000

Fig. 4.

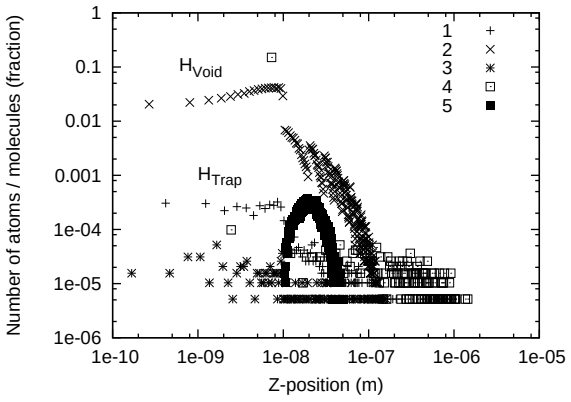
HVoid
HTrap
1
2
3
4
5
Number of atoms / molecules (fraction)
Z-position (m)
1
0.1
0.01
0.001
1e-04
1e-05
1e-06
1e-10
1e-09
1e-08
1e-07
1e-06
1e-05

Fig. 5.